

A comparative study on charge carrier recombination across the junction region of Cu₂ZnSn(S,Se)₄ and Cu(In,Ga)Se₂ thin film solar cells

著者別名	イスラム ムハマド モニルル, 櫻井 岳暁
journal or publication title	AIP Advances
volume	6
number	3
page range	035216
year	2016-03
権利	(C) 2016 Author(s). All article content, except where otherwise noted, is licensed under a Creative Commons Attribution (CC BY) license
URL	http://hdl.handle.net/2241/00142125

doi: 10.1063/1.4944911



A comparative study on charge carrier recombination across the junction region of $\text{Cu}_2\text{ZnSn}(\text{S},\text{Se})_4$ and $\text{Cu}(\text{In},\text{Ga})\text{Se}_2$ thin film solar cells

Mohammad Abdul Halim, Muhammad Monirul Islam, Xianjia Luo, Takeaki Sakurai, Noriyuki Sakai, Takuya Kato, Hiroki Sugimoto, Hitoshi Tampo, Hajime Shibata, Shigeru Niki, and Katsuhiko Akimoto

Citation: *AIP Advances* **6**, 035216 (2016); doi: 10.1063/1.4944911

View online: <http://dx.doi.org/10.1063/1.4944911>

View Table of Contents: <http://scitation.aip.org/content/aip/journal/adva/6/3?ver=pdfcov>

Published by the *AIP Publishing*

Articles you may be interested in

[Microstructural analysis of 9.7% efficient \$\text{Cu}_2\text{ZnSnSe}_4\$ thin film solar cells](#)

Appl. Phys. Lett. **105**, 183903 (2014); 10.1063/1.4901401

[The impact of oxygen incorporation during intrinsic ZnO sputtering on the performance of \$\text{Cu}\(\text{In},\text{Ga}\)\text{Se}_2\$ thin film solar cells](#)

Appl. Phys. Lett. **105**, 083906 (2014); 10.1063/1.4894214

[Intermixing at the absorber-buffer layer interface in thin-film solar cells: The electronic effects of point defects in \$\text{Cu}\(\text{In},\text{Ga}\)\(\text{Se},\text{S}\)_2\$ and \$\text{Cu}_2\text{ZnSn}\(\text{Se},\text{S}\)_4\$ devices](#)

J. Appl. Phys. **116**, 063505 (2014); 10.1063/1.4892407

[Employing time-resolved terahertz spectroscopy to analyze carrier dynamics in thin-film \$\text{Cu}_2\text{ZnSn}\(\text{S},\text{Se}\)_4\$ absorber layers](#)

Appl. Phys. Lett. **104**, 253901 (2014); 10.1063/1.4884817

[Loss mechanisms in hydrazine-processed \$\text{Cu}_2\text{ZnSn}\(\text{Se},\text{S}\)_4\$ solar cells](#)

Appl. Phys. Lett. **97**, 233506 (2010); 10.1063/1.3522884

The advertisement features a large image of a water droplet on the left, with the word 'COMPUTATIONAL' and 'SCIENCE ENGINEERING' faintly visible in the background. On the right, there is a small image of the 'Computational Science and Engineering' journal cover, which includes the text 'Scientific Software Communities' and the IEEE logo. To the right of the journal cover, the text reads: 'Broaden your impact to scientists and engineers in 50+ societies. Submit your computational article to CISE.'

A comparative study on charge carrier recombination across the junction region of $\text{Cu}_2\text{ZnSn}(\text{S},\text{Se})_4$ and $\text{Cu}(\text{In},\text{Ga})\text{Se}_2$ thin film solar cells

Mohammad Abdul Halim,^{1,a} Muhammad Monirul Islam,¹ Xianjia Luo,¹ Takeaki Sakurai,¹ Noriyuki Sakai,² Takuya Kato,² Hiroki Sugimoto,² Hitoshi Tampo,³ Hajime Shibata,³ Shigeru Niki,³ and Katsuhiko Akimoto¹

¹Institute of Applied Physics, University of Tsukuba, Tsukuba, Ibaraki 305-8573, Japan

²Energy Solution Business Center, Showa Shell Sekiyu K.K., Minato, Tokyo 135-8074, Japan

³National Institute of Advanced Industrial Science and Technology (AIST), Tsukuba, Ibaraki 305-8568, Japan

(Received 12 January 2016; accepted 14 March 2016; published online 23 March 2016)

A comparative study with focusing on carrier recombination properties in $\text{Cu}_2\text{ZnSn}(\text{S},\text{Se})_4$ (CZTSSe) and the CuInGaSe_2 (CIGS) solar cells has been carried out. For this purpose, electroluminescence (EL) and also bias-dependent time resolved photoluminescence (TRPL) using femtosecond (fs) laser source were performed. For the similar forward current density, the EL-intensity of the CZTSSe sample was obtained significantly lower than that of the CIGS sample. Primarily, it can be attributed to the existence of excess amount of non-radiative recombination center in the CZTSSe, and/or CZTSSe/CdS interface comparing to that of CIGS sample. In case of CIGS sample, TRPL decay time was found to increase with the application of forward-bias. This can be attributed to the reduced charge separation rate resulting from the reduced electric-field at the junction. However, in CZTSSe sample, TRPL decay time has been found almost independent under the forward and reverse-bias conditions. This phenomenon indicates that the charge recombination rate strongly dominates over the charge separation rate across the junction of the CZTSSe sample. Finally, temperature dependent V_{OC} suggests that interface related recombination in the CZTSSe solar cell structure might be one of the major factors that affect EL-intensity and also, TRPL decay curves. © 2016 Author(s). All article content, except where otherwise noted, is licensed under a Creative Commons Attribution (CC BY) license (<http://creativecommons.org/licenses/by/4.0/>). [<http://dx.doi.org/10.1063/1.4944911>]

I. INTRODUCTION

The second generation thin film solar cells based on chalcopyrite $\text{Cu}(\text{In},\text{Ga})\text{Se}_2$ (CIGS) are already in the commercial stage. Currently, among the thin film solar cells, the world record power conversion efficiency of lab-scale CIGS is 21.7%.¹ However, non-abundant and/or expensive elements, In and Ga are considered as obstacles to meet future multi-terawatt-scale global energy demand.^{2,3} Replacing In and Ga in CIGS with earth-abundant Zn and Sn, we can obtain $\text{Cu}_2\text{ZnSn}(\text{S}_x\text{Se}_{1-x})_4$ (CZTSSe) which has drawn increased attention as an alternative absorber layer.⁴⁻⁹ CZTSSe has optimal band gap (1.0–1.5 eV, depending on the S, Se compositions),¹⁰ and also high absorption coefficient ($\sim 10^4 \text{ cm}^{-1}$) that make it suitable for solar cell application.¹¹ Nevertheless, the highest achieved efficiency, so far, using CZTSSe is 12.6%,¹² which is only about half of the similar structured CIGS-based solar cell. Among the solar cell parameters, poor open circuit voltage (V_{OC}) i.e., large V_{OC} -deficiency ($E_g/q - V_{OC}$) is considered as the primary limiting factor to achieve the highest possible efficiency in CZTSSe-based solar cells.¹³ Therefore, further progress

^aE-mail: halimtsukuba2012@gmail.com



for the CZTSSe based solar cells mostly depends on the deeper understanding of the defects that lower the V_{OC} relative to its Shockley-Queisser value.¹⁴

Although many factors can affect the V_{OC} of a solar cell, the charge-carrier recombination in the junction-region may be dominant. Generally an improvement in the V_{OC} depends on how slowly the photo-generated carriers recombine with time. Therefore it is crucial to understand charge carrier generation, recombination, and more importantly the separation of these charge carriers by the internal electric-field produced in the junction-region. Photoluminescence (PL) spectroscopy is a widely used technique to study carrier recombination process in the CIGS materials as well as CZTSSe.¹⁵⁻²¹ However, to investigate the junction quality of the semiconductors, electroluminescence (EL) proves to be useful.²²⁻²⁵ Nevertheless, EL-spectroscopy the principle of which is the exact inverse of the photovoltaic principle has never been used for CZTSSe material systems so far, although there have been some reports for CIGS materials.^{22,23} In the present study we have compared the charge carrier recombination process across the junction regions of CZTSSe and highly efficient CIGS solar cells. For this purpose, room temperature EL and time resolved photoluminescence (TRPL) under different external bias have been investigated. A combined study of the EL and TRPL is crucial to understand the complete carrier recombination mechanism of both the CIGS and the CZTSSe material.

II. EXPERIMENTAL

The CZTSSe thin-film solar cell was fabricated at Solar Frontier, Japan. In the cell structure, the absorber layer of CZTSSe was grown by sulfo-selenization after forming of metallic precursor stacking by co-sputtering method over a Mo coated soda lime glass substrate. The compositions of the grown CZTSSe film have been found as $[Cu]/[Sn] \sim 1.77$ and $[Se]/[S+Se] \sim 0.85$ as estimated from the electron probe microanalysis (EPMA). The band gap was estimated to be ~ 1.10 eV as calculated from the external quantum efficiency data. The CIGS solar cell has been fabricated at the National Institute of Advanced Industrial Science and Technology (AIST), Japan. CIGS film was grown by a three-stage process using a molecular beam epitaxy (MBE) system.²⁶ The $[Ga]/[In+Ga]$ ratio of the CIGS sample has been found to be ~ 0.30 which is also estimated by EPMA. All of these measurements of EL, TRPL and temperature dependent V_{OC} were performed on the solar cell structures. A Keithley 2635B source meter has been used as an injection current source for the EL measurement and also as a voltage source for the external bias dependent TRPL measurement. In TRPL, photo-excitation was carried out by a mode-locked titanium: sapphire laser with the wavelength of 750 nm and luminescence signals were detected by an InGaAs based photomultiplier detector. The laser output comprised of 2 and 4 MHz pulse train with a pulse width of ~ 80 femtosecond (fs). The diameter of the laser spot on the sample was approximately $70 \mu\text{m}$ and the photon density per pulse was approximately 10^{11} photons. cm^{-2} and it was chosen for excess carrier injection.

III. RESULTS AND DISCUSSION

EL spectra measured at RT for the CIGS and the CZTSSe devices are presented in the Fig. 1(a) and 1(b), respectively. The injection current of the measurements was fixed at 2253 mAcm^{-2} and 2546 mAcm^{-2} , for the CIGS and the CZTSSe sample, respectively. It should be mentioned here that the conduction band off-set between the *n*-type CdS window and the CZTSSe (*p*-type) is significantly smaller ($\Delta E_C \sim 0.4$ eV) than that of the valence band off-set ($\Delta E_V \sim 1.0$ eV).²⁷ Almost similar type of band alignment between CdS and CIGS has also been reported.²⁸ Therefore, considering the above condition, during EL measurement, as the forward bias flattens the conduction band edge, electrons can easily be injected into the lower gap *p*-type absorber layers (both in the CZTSSe and the CIGS). On the contrary, the higher valence band off-set between the CdS and the CZTSSe or CIGS blocks the injection of holes from *p*-type absorber to *n*-type window material. Obviously, due to the injection of excess minority carriers in the absorber layer, recombination will take place in the lower gap region. As the recombination of these excess carriers occurs very near the metallurgical junction region, quality of both the interface and the depletion region can affect the recombination mechanisms, therefore, the EL-intensity. It should be noted that, during EL measurement, although

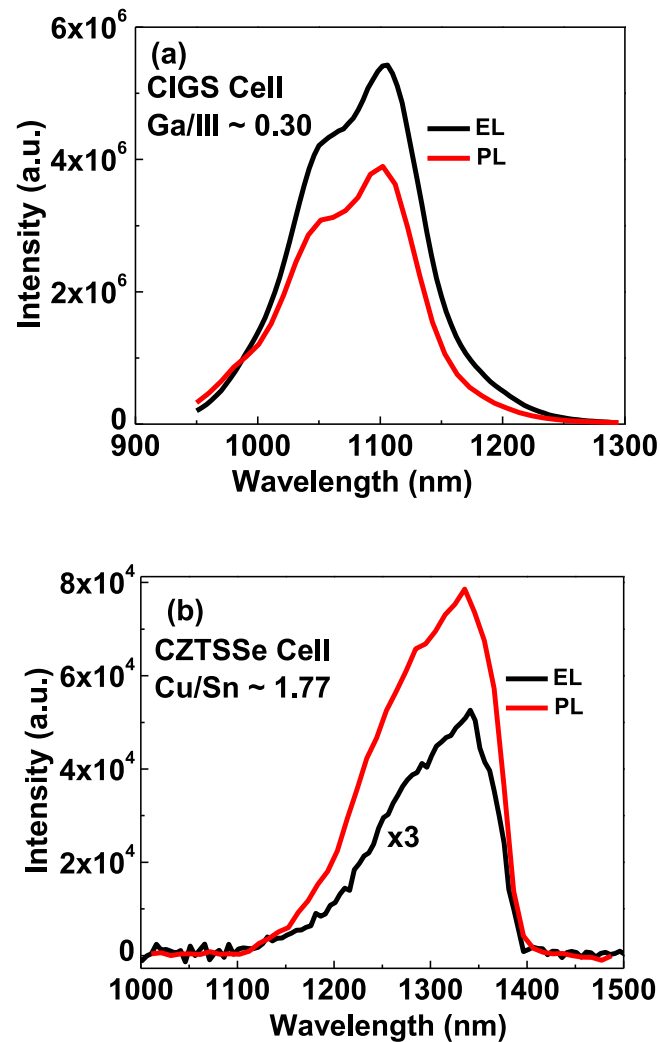


FIG. 1. Room temperature EL and PL spectra for (a) CIGS and (b) CZTSSe solar cells.

the injection current was slightly higher for CZTSSe sample, corresponding EL intensity is more than two orders of magnitude lower than that of CIGS device (see the vertical scale of Fig. 1). It suggests the existence of excess amount of non-radiative recombination centers in the CZTSSe and/or CdS/CZTSSe interface comparing to that of the CIGS sample. Together with the EL spectra, the PL spectra of both the CZTSSe and CIGS samples measured under similar optical excitation are also shown in figure 1. It is interesting to note that the same peak position in both the EL and PL spectra for the CZTSSe and also for CIGS sample. It suggests, the origin of the luminescence are due to the similar electronic transition.

The performance of studied samples are given in table I. Although the band gap of both the CZTSSe and the CIGS are comparable, there is significant decrease in the V_{OC} of the CZTSSe solar cell. The loss of V_{OC} can be attributed to the enhanced non-radiative recombination in the CZTSSe sample which is also reflected in the reduced EL-intensity as mentioned above.

TABLE I. Device characteristics of CZTSSe and CIGS solar cells under AM 1.5 G illumination.

Sample	Eff (%)	V_{OC} (mV)	J_{SC} (mA/cm ²)	FF (%)	E_g (eV)
CZTSSe	5.2	397	33.6	38.8	~1.10
CIGS	15.9	681	34.0	69.0	~1.15

To understand more about the quantitative idea of the carrier-recombination mechanism, we have performed TRPL from which effective decay time can be estimated. The measured TRPL decay curves for the CdS/(CZTSSe or CIGS) and ZnO/CdS/(CZTSSe or CIGS) structures are shown in Fig. 2. An ultrafast laser with pulse-width ~ 80 fs, and the wavelength of 750 nm has been used as an excitation source for the TRPL measurement. The corresponding photon energy (1.65 eV) of the laser excitation is lower than the band-gap energy of the CdS (2.42 eV) and the ZnO (3.35 eV).²⁹ Therefore, light will be transmitted through these layers and will be absorbed only in the CZTSSe or CIGS layer in the structure. From the transmittance and reflectance data we have estimated that the absorption coefficients of the studied CZTSSe and CIGS for the wavelength of 750 nm are 4×10^4 and 3.8×10^4 cm^{-1} respectively (data not shown here). Taking into account similar absorption coefficient and the band-gap energy of the CZTSSe and CIGS layers in this study, we can consider the penetration depth of the 750 nm excitation in both samples is almost similar. The decay curves could be fitted by a double-exponential function:

$$I_{PL}(t) = C_1 e^{-t/\tau_1} + C_2 e^{-t/\tau_2}, \quad (1)$$

where t is the time after a laser pulse excitation, $I(t)$ is the luminescence intensity at time t , C_1 and C_2 are PL intensities of the corresponding PL components, and τ_1 and τ_2 are the fast and slow decay

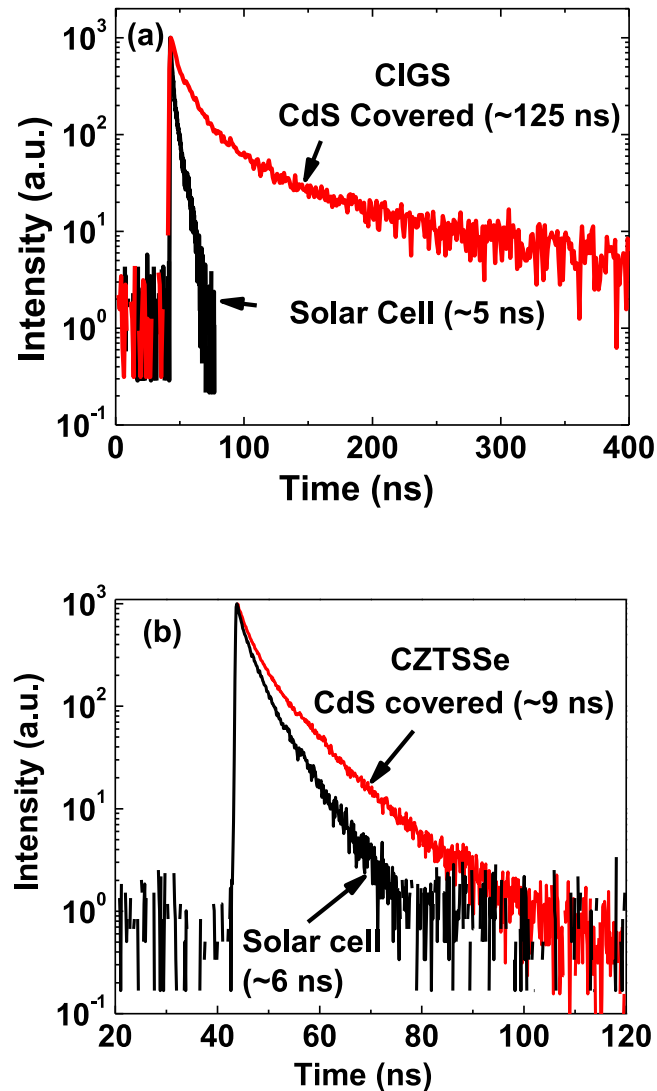


FIG. 2. TRPL decay curves for CdS covered and solar cell structure of (a) CIGS and (b) CZTSSe samples.

lifetimes. In our study, τ_2 is considered as an effective decay time for comparison, which is relevant for solar cell operation. For the determination of the decay time a single exponential fit in the slow decay avoiding the fast initial decay has been used. In general, the effective decay time, τ_{eff} can be expressed as

$$\frac{1}{\tau_{eff}} = \frac{1}{\tau_r} + \frac{1}{\tau_{nr}}, \quad (2)$$

where τ_r is the radiative lifetime and τ_{nr} is the non-radiative lifetime of the carriers.³⁰ In case of a *p-n* junction, some of the excited carriers can be drifted out of the depletion region by the built-in electric field at the junction before recombination. Thus, the population of the available excited carriers becomes less which would otherwise be recombined with time. Consequently, TRPL decay curve becomes faster, and hence yields smaller decay time. Therefore, in case of the *p-n* junction, τ_{eff} can be expressed as

$$\frac{1}{\tau_{eff}} = \frac{1}{\tau_r} + \frac{1}{\tau_{nr}} + \frac{1}{\tau_{drift}}, \quad (3)$$

where τ_{drift} is the carrier drift-out time at the junction. From the Fig. 2 at first, it is apparent that decay time in the CdS covered CIGS layer is ~ 125 ns which is much higher comparing to that of CdS covered CZTSSe layer (~ 9 ns). It usually suggests that non-radiative recombination in CZTSSe is significantly higher comparing to CIGS. Another noteworthy observation is that in case of CIGS, decay time has been significantly reduced to 5 ns for the ZnO/CdS/CIGS structure comparing to that of CdS covered CIGS (~ 125 ns). It indicates that τ_{eff} strongly depends on the τ_{drift} . It has been reported that ZnO, combined with CdS, makes strong electric-field at the ZnO/CdS/CIGS structure and this electric-field quickly reduces the population of photo-generated carriers across the junction.³¹ As a result, PL intensity abruptly falls resulting in extremely lower TRPL decay time. On the other hand, decay time remains almost similar in both the CdS covered CZTSSe and ZnO/CdS/CZTSSe structure. This phenomenon can also be attributed to the existence of large amount of defect states at the CdS/CZTSSe interface and/or bulk of the CZTSSe layer. These defect states act as more efficient recombination centers whose carrier capture-time is faster than the carrier drifting time by the internal electric-field. Therefore, we may argue that in CZTSSe solar cell τ_{nr} still remains dominant over τ_{drift} unlike the CIGS case.

To investigate more quantitatively about the effect of the electric-field on the carrier dynamics, we have studied bias dependent TRPL for the ZnO/CdS/CZTSSe (or CIGS) structures. The pulse laser excited carrier recombination dynamics under different bias conditions are shown in the Fig. 3. As can be seen in figure 3(a), in case of the CIGS solar cells, the forward bias significantly increases the decay time and also reverse bias produces shorter decay time as expected. The increase of the decay time under forward bias condition in CIGS solar cell structure has also been reported by other groups.^{32,33} As we have explained before, without applying external bias, photo-excited excess-carriers are separated by the electric-field in the junction due to built-in voltage. With the application of forward bias, the electric-field in the junction-region is reduced, and then carrier-separation becomes less effective resulting in the longer decay time. On the other hand, reverse bias produces strong electric-field across the junction that enhances charge separation due to high carrier drift velocity. However, TRPL decay curves for the CZTSSe sample seems to be independent on the external bias conditions as can be seen in Fig. 3(b). It suggests τ_{drift} , is unaffected. The estimated TRPL decay times measured under different external bias (forward and reverse) conditions are summarized in table II. As we can see, in CIGS the estimated decay time significantly depends on biasing, whereas in CZTSSe it is almost independent on biasing. The results, therefore, justify our explanation that the CZTSSe contains high concentration of recombination center whose capture time is faster than the separation time of the photo-generated carriers near the depletion region.

To understand whether the carrier recombination mechanism is more active at the interface states, temperature-dependent V_{OC} measurement has been performed for both the CIGS and the CZTSSe structure (Fig. 4). The V_{OC} is related with the temperature, T as follows,³⁴

$$V_{OC} = \frac{E_A}{q} - \frac{AkT}{q} \times \ln \left(\frac{J_{00}}{J_{SC}} \right), \quad (4)$$

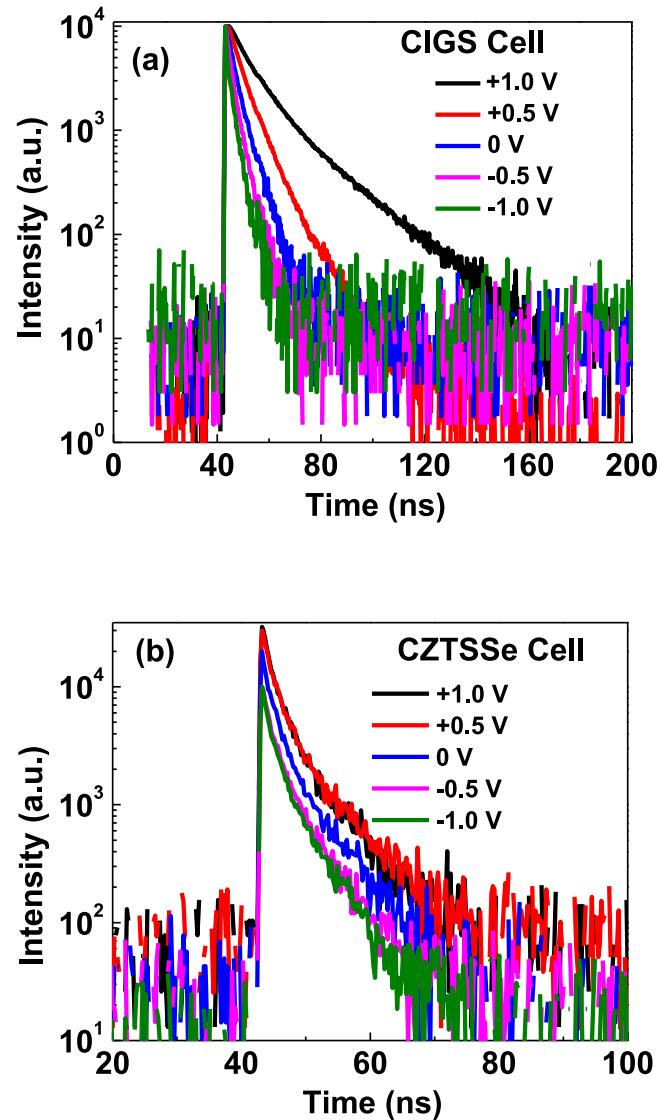


FIG. 3. TRPL decay curves for (a) CIGS and (b) CZTSSe solar cells under different external voltages. The applied voltages were 1.0 V, 0.5 V, 0 V, -0.5 V and -1.0 V.

where E_A , A , k , J_{00} and J_{SC} are the activation energy of the dominant recombination, diode ideality factor, Boltzmann constant, reverse saturation current prefactor, and short circuit current density, respectively. Considering A , J_{SC} and J_{00} in Eq. (3) are independent of the T , a plot of V_{OC} vs T should yield a straight line, and the extrapolation of this line to $T=0$ K gives the activation energy E_A . It has been reported that if Shockly-Read-Hall (SRH) recombination mechanism dominates in the depletion region then E_A will be equal to the band-gap, E_g of the corresponding absorber layer.³⁵

TABLE II. The measured TTRPL decay time for CZTSSe and CIGS devices under different external biasing.

Bias Voltage	Decay time in CIGS device (ns)	Decay time in CZTSSe device (ns)
+1.0 V	21.3	7.2
+0.5 V	12.7	6.3
0 V	5.1	6.4
-0.5 V	4.4	5.8
-1.0 V	3.3	5.2

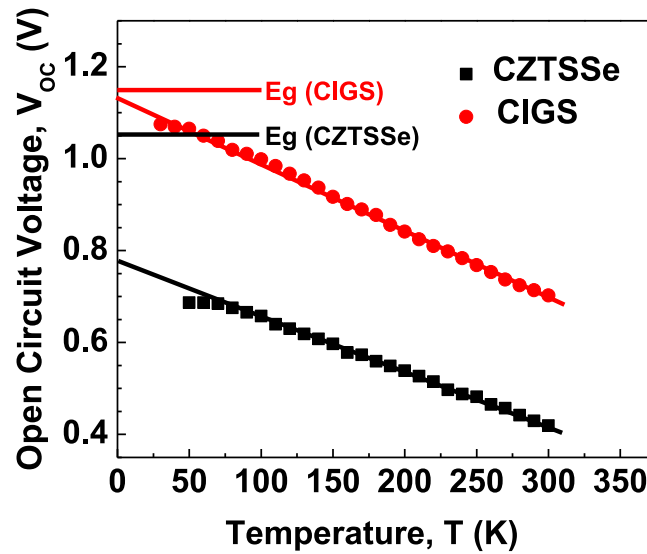


FIG. 4. Temperature dependent open circuit voltage for CIGS and CZTSSe solar cells from which activation energy of the dominant recombination was calculated.

On the other hand, if E_A is smaller than E_g , it indicates buffer-absorber interface recombination more dominant.^{36,37} In case of CZTSSe structure, from the V_{OC} vs T data we estimated E_A value to be around 0.8 eV which is less than the CZTSSe band-gap of 1.10 eV. Such kind of lower E_A value suggests that the interface-recombination is more dominant than the recombination at the depletion region of the CZTSSe absorber layer. On the other hand, in case of CIGS structure the E_A is almost equal to the E_g of CIGS indicating SRH recombination in the depletion region is more dominant. Of course, we can not exclude recombination due to localized states at the bulk region, however, from the above experiments, it seems interface-related recombination is one of the major factors that affects the carrier recombination dynamics in the CZTSSe device comparing to that of CIGS device.

IV. CONCLUSIONS

We have performed electroluminescence, bias dependent TRPL, and temperature dependent V_{OC} on the CZTSSe and the CIGS solar cells. A significant decrease in the EL-intensity for the CZTSSe comparing to CIGS indicates excess non-radiative recombination centers in the CZTSSe sample. For a CIGS solar cell, carrier recombination rates are observed to be decreased and increased under forward and reverse bias respectively, i.e. TRPL decay curves are strongly dependent on the external bias voltage. Such kind of carrier recombination behaviors are expected in case of an ideal $p-n$ junction solar cell. However, in case of the CZTSSe solar cell, the TRPL decay curves seems to be unaffected under the external bias conditions. These results were attributed to the increased recombination at the interface and/or at the bulk of the CZTSSe. Finally, the temperature dependent open circuit voltage suggests that recombination at the CdS/CZTSSe interface is might be more active in the CZTSSe solar cell structure than CdS/CIGS.

ACKNOWLEDGEMENT

This work is supported by the New Energy and Industrial Technology Development Organization (NEDO) and the Ministry of Economy, Trade and Industry of Japan (METI).

¹ P. Jackson, D. Hariskos, R. Wuerz, O. Kiowski, A. Bauer, T. M. Friedlmeier, and M. Powalla, *Phys. Status Solidi (RRL)* **9**, 28 (2015).

² C. Wadia, A. P. Alivisatos, and D. M. Kammen, *Environ. Sci. Technol.* **43**, 2072 (2009).

³ B. A. Andersson, *Prog. Photovoltaics: Res. Appl.* **8**, 61 (2000).

- ⁴ T. Tanaka, T. Nagatomo, D. Kawasaki, M. Nishio, Q. Guo, A. Wakahara, A. Yoshida, and H. Ogawa, *J. Phys. Chem. Sol.* **66**, 1978 (2005).
- ⁵ H. Katagiri, K. Jimbo, S. Yamada, T. Kamimura, W. S. Maw, T. Fukano, T. Ito, and T. Motohiro, *Appl. Phys. Express* **1**, 041201 (2008).
- ⁶ N. Nakayama and K. Ito, *Appl. Surf. Sci.* **92**, 171 (1996).
- ⁷ A. Weber, S. Schmidt, D. Abou-Ras, P. Schubert-Bischoff, I. Denks, R. Mainz, and H. W. Schock, *Appl. Phys. Lett.* **95**, 041904 (2009).
- ⁸ S. C. Riha, B. A. Parkinson, and A. L. Prieto, *J. Am. Chem. Soc.* **131**, 12054 (2009).
- ⁹ S. Siebentritt and S. Schorr, *Prog. Photovoltaics: Res. Appl.* **20**, 512 (2012).
- ¹⁰ S. Chen, X. G. Gong, A. Walsh, and S. H. Wei, *Applied Physics Letters* **94**, 041903 (2009).
- ¹¹ J. S. Seol, S. Y. Lee, J. C. Lee, H. D. Nam, and K. H. Kim, *Sol. Energy Mater. Sol. Cells* **75**, 155 (2003).
- ¹² W. Wang, M. T. Winkler, O. Gunawan, T. Gokmen, T. K. Todorov, Y. Zhu, and D. B. Mitzi, *Adv. Energy Mater.* **4**, 1301465 (2014).
- ¹³ D. B. Mitzi, O. Gunawan, T. K. Todorov, K. Wang, and S. Guha, *Sol. Energy Mater. Sol. Cells* **95**, 1421 (2011).
- ¹⁴ W. Shockley and H. J. Queisser, *J. Appl. Phys.* **32**, 510 (1961).
- ¹⁵ S. Siebentritt, in *Wide-Gap Chalcopyrites*, edited by S. Siebentritt and U. Rau (Springer, Heidelberg, 2006), Chap. 7.
- ¹⁶ W. K. Metzger, I. L. Repins, M. Romero, P. Dippo, M. Contreras, R. Noufi, and D. Levi, *Thin Solid Films* **517**, 2360 (2009).
- ¹⁷ S. Shimakawa, K. Kitani, S. Hayashi, T. Satoh, Y. Hashimoto, Y. Takahashi, and T. Negami, *Phys. Status Solidi A* **203**, 2630 (2006).
- ¹⁸ S. Shirakata and T. Nakada, *Thin Solid Films* **515**, 6151 (2007).
- ¹⁹ X. Lin, A. Ennaoui, S. Levchenko, T. Dittrich, J. Kavalakkath, S. Kretschmar, T. Unold, and M. Ch. Lux-Steiner, *Appl. Phys. Lett.* **106**, 013903 (2015).
- ²⁰ M. Grossberg, J. Krustok, K. Timmo, and M. Altosaar, *Thin Solid Films* **517**, 2489 (2009).
- ²¹ K. Tanaka, Y. Miyamoto, H. Uchiki, K. Nakazawa, and H. Araki, *Phys. Status Solidi A* **203**, 2891 (2006).
- ²² T. Kirchartz and U. Rau, *J. Appl. Phys.* **102**, 104510 (2007).
- ²³ T. Kirchartz, U. Rau, M. Kurth, J. Matheis, and J. H. Werner, *Thin Solid Films* **515**, 6238 (2007).
- ²⁴ P. M. Bridenbaugh and P. Migliorato, *Appl. Phys. Lett.* **26**, 459 (1975).
- ²⁵ P. Migliorato and J. I. Shay, *J. Appl. Phys.* **46**, 1777 (1975).
- ²⁶ S. Ishizuka, K. Sakurai, A. Yamada, K. Matsubara, P. Fons, K. Iwata, S. Nakamura, Y. Kimura, T. Baba, H. Nakanishi, T. Kojima, and S. Niki, *Sol. Energy Mater. Sol. Cells* **87**, 541 (2005).
- ²⁷ R. Haight, A. Barkhouse, O. Gunawan, B. Shin, M. Copel, M. Hopstaken, and D. V. Mitzi, *Appl. Phys. Lett.* **98**, 253502 (2011).
- ²⁸ T. Minemoto, T. Matsui, H. Takakura, Y. Hamakawa, T. Negami, Y. Hashimoto, T. Uenoyama, and M. Kitagawa, *Sol. Energy Mater. Sol. Cells* **67**, 83 (2001).
- ²⁹ S. M. Sze, *Semiconductor devices: Physics and Technology*, 2nd ed., p. 537.
- ³⁰ J. I. Pankove, *Optical Processes in Semiconductors* (Dover, New York, 1971).
- ³¹ W. K. Metzger, I. L. Repins, and M. A. Contreras, *Appl. Phys. Lett.* **93**, 022110 (2008).
- ³² D. Kuciauskas, J. V. Li, A. Kanevce, H. Guthrey, M. Contreras, J. Pankow, P. Dippo, and K. Ramanathan, *J. Appl. Phys.* **117**, 185102 (2015).
- ³³ M. Maiberg, C. Spindler, E. Jarzembowski, and R. Scheer, *Thin Solid Films* **582**, 379 (2015).
- ³⁴ V. Nadenau, U. Rao, A. Jasenek, and H. W. Schock, *J. Appl. Phys.* **87**, 584 (2000).
- ³⁵ S. S. Hegedus and W. N. Shafarman, *Prog. Photovoltaics: Res. Appl.* **12**, 155 (2004).
- ³⁶ O. Gunawan, T. K. Todorov, and D. V. Mitzi, *Appl. Phys. Lett.* **97**, 233506 (2010).
- ³⁷ K. Wang, O. Gunawan, T. Todorov, B. Shin, S. J. Chey, N. A. Bojarczuk, D. Mitzi, and S. Guha, *Appl. Phys. Lett.* **97**, 143508 (2010).